ELSEVIER

Journal of Photochemistry and Photobiology A: Chemistry 106 (1997) 27–30

Journal of PHOTOCHEMISTRY AND PHOTOBIOLOGY A: CHEMISTRY

Pulsed laser ablation of polyimide: fundamental aspects

D. Bäuerle *, M. Himmelbauer, E. Arenholz

Angewandte Physik, Johannes-Kepler-Universität Linz, A-4040 Linz, Austria

Abstract

Single-shot laser ablation of polyimide in air was investigated using focused Ar^+ laser UV radiation ($\lambda \approx 302$ nm) and pulse lengths between 140 ns and 5 μs. The irradiated polymer surface was studied in terms of its topology and ablation depth by atomic force microscopy. The dependence of the ablation threshold on the laser pulse length and intensity can be tentatively interpreted on the basis of a thermal process and a (thermal or non-thermal) mechanism which decreases the apparent activation energy for the desorption of species from the surface. On the basis of the changes in surface topology observed, a new model for the formation of interference gratings and row doubling is suggested.

Keywords: Fundamental aspects; Polyimide; Pulsed laser ablation

1. Introduction

Material removal caused by short, high-intensity laser pulses is often called pulsed laser ablation. Today, this technique is employed for the surface patterning of brittle and heat-sensitive materials and for the fabrication of thin films [1]. In spite of the large number of experimental and theoretical investigations performed, the mechanisms involved in pulsed laser ablation are still unclear in many systems. For example, for the UV laser ablation of organic polymers, the relative importance of thermal and non-thermal mechanisms, including defect and stress formation, is still unknown [1–6]. So far, UV laser ablation of organic polymers has been studied mainly using excimer lasers with typical pulse lengths of 10–40 ns [1,2] and with chopped or scanned continuous wave (cw) lasers with dwell times of 10 μs or more [7–9]. In these investigations, multiple pulse ablation rates have been studied mainly as a function of the laser fluence ϕ. However, for the determination of the basic interaction mechanisms, it is desirable to know the dependence of the ablation rate on the laser intensity at constant pulse length, and vice versa.

In a series of foregoing papers, we have presented the first systematic investigations of the surface topology changes and ablation of polyimide (PI) observed under focused UV laser irradiation [10–12]. In this case, the laser beam intensity I and the pulse length τ_l are independently varied via the fluence $\phi = I\tau_l$. In order to separate the basic interaction mechanisms from the physical and chemical changes related to multiple pulse irradiation, we have performed single-shot experiments. For these reasons, the changes in surface topology and ablation depth can be studied by atomic force microscopy (AFM) only. In contrast with mass loss measurements using a quartz crystal microbalance (QCM), the present technique permits the investigation with high accuracy of the real surface profile near the threshold fluence for ablation ϕ_{th}.

2. Experimental details

The experimental details have been given in Ref. [10]. The PI foils (Kapton H, DuPont, 50 μm thick) employed in the experiments were mainly amorphous with about 10 vol.% crystalline domains. The foils were irradiated in air by an externally pulsed cw Ar^+ laser operating in the UV region (TEM_{00} mode). The spectral distribution consisted of a pronounced maximum at a centre wavelength $\lambda_C = 302$ nm ($\Delta\lambda = 9$ nm) and a less intense peak at around 275 nm. Rectangular laser pulses with pulse lengths τ_l of 140 ns to 5 μs (full width at half-maximum, FWHM) were generated by a digitally driven acousto-optic modulator. The focal spot size was $2w_0 = 4.2 \pm 0.4$ μm. The fluence on the polymer surface was of gaussian shape, i.e. $\phi(r) = \phi_0 \exp[-(r/w_0)^2]$. The surface topology of the sample was investigated using an atomic force microscope in the contact mode. The lateral and vertical resolutions were 30 nm and 1 nm respectively.

* Corresponding author. Tel.: +43 732 2468; fax: +43 732 2468/9242

1010-6030/97/$17.00
PII S1010-6030(97)00034-8

3. Results and discussion

Fig. 1 shows AFM pictures of the polymer surface irradiated with laser fluences $\phi_0 \leq \phi_{th}$, $\phi_0 \geq \phi_{th}$ and $\phi_0 > \phi_{th}$. These regimes will now be discussed separately.

3.1. Fluences $\phi_0 \leq \phi_{th}$

With centre fluences $\phi_0 \leq \phi_{th}$, the irradiated area shows a hump which is surrounded by a depression (Fig. 1(a)). The increase in specific volume (approximately 10% for $\tau_l = 200$ ns and $\phi_0 \approx 0.96\phi_{th}$) which results in hump formation cannot be explained solely by the amorphization of crystalline domains ($\rho_C/\rho_A = 1.11 \pm 0.02$ [13,14]). Therefore we suggest that (large) fragments which are generated by thermal or non-thermal processes, and which are trapped within the polymer, contribute to the volume increase. Small fragments, such as CO, CN, C, C_2, CH, C_2H_2, etc., are released from the sample [15].

The formation of the depression may originate from plastic deformation. Residual stresses generated within the foil during manufacturing cause PI to shrink on first exposure to elevated temperatures. Laser-induced heating may therefore cause lateral stress relaxation and material redistribution, forming a depression on the surface. Near the centre of the irradiated spot, this effect is overcompensated by the increase in specific volume.

3.2. Fluences $\phi_0 \geq \phi_{th}$

The surface topology observed with fluences $\phi_0 \geq \phi_{th}$ is shown in Fig. 1(b). The top of the hump now shows a dip

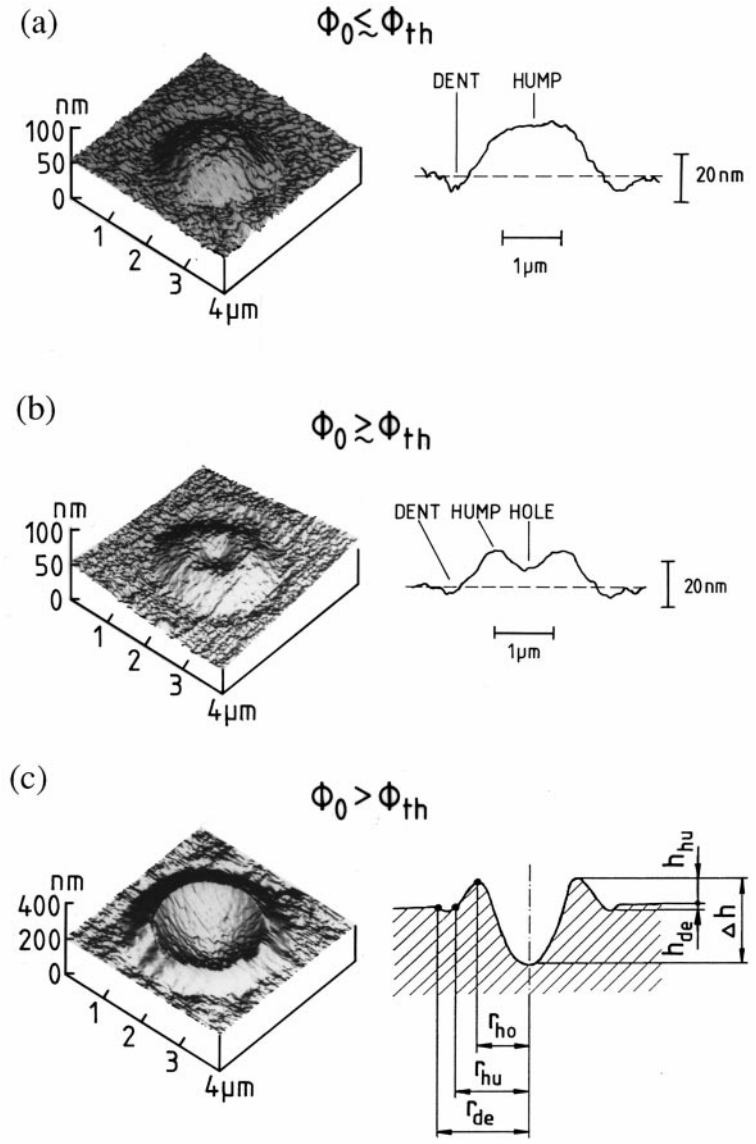

Fig. 1. UV laser-induced surface topology changes on PI. The fluence on the polymer surface was of gaussian shape ($\phi(r) = \phi_0 \exp[-(r/w_0)^2]$) with $w_0 \approx$ 2.1 μm. Left: AFM pictures (three-dimensional view). Right: cross-sections. (a,b) AFM pictures; (c) schematic picture; (a) $\phi_0/\phi_{th} \approx 0.96$ and $\tau_l = 5$ μs; (b) $\phi_0/\phi_{th} \approx 1.01$ and $\tau_l = 2.1$ μs; (c) $\phi_0/\phi_{th} \approx 1.25$ and $\tau_l = 800$ ns.

(hole) which is due to material ablation. Subsequently, we define the threshold fluence for ablation by the average of the lowest fluence at which a dip appears in the centre of the hump and the highest fluence for which this dip is absent. For a fixed pulse length and within the range 140 ns $\leq \tau_l \leq$ 5 μs, we find $\phi_{th} \propto \tau_l^{\epsilon}$ with $\epsilon \approx 0.36$ (Fig. 2).

With a *photochemical* process, ablation should depend on the dose only, and we would expect ϕ_{th} = constant. If, on the other hand, we assume a *thermal* process, ablation should start, in a first approximation, at around the same threshold temperature $T_{th} \equiv T(\phi_{th})$ = constant. If the heat penetration depth exceeds the optical penetration depth, i.e. if $l_T \gg l_\alpha$, a crude approximation yields $\phi_{th} \propto \tau_l^{\epsilon}$ with $\epsilon = 0.5$ [1]. If $l_T \ll l_\alpha$, the fluence ϕ_{th} becomes independent of τ_l, i.e. $\epsilon = 0$. A more rigorous estimate of the maximum surface temperature shows that we obtain for all pulse lengths, together with the corresponding threshold fluences derived from the experiments, the same centre temperature, 1300 ± 50 K [10].

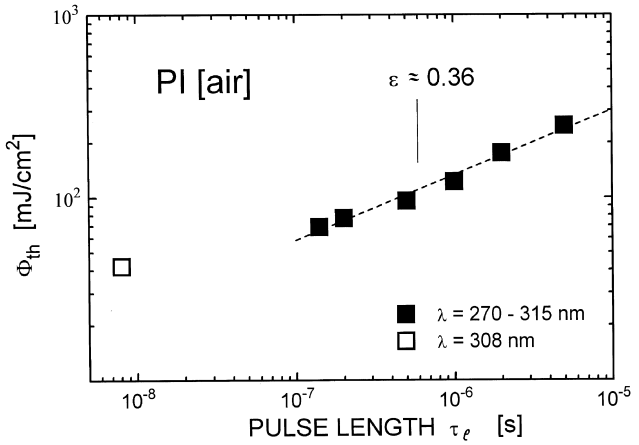

Fig. 2. Dependence of the threshold fluence for ablation ϕ_{th} on the laser pulse length τ_l: ■, this work; □, Ref. [16].

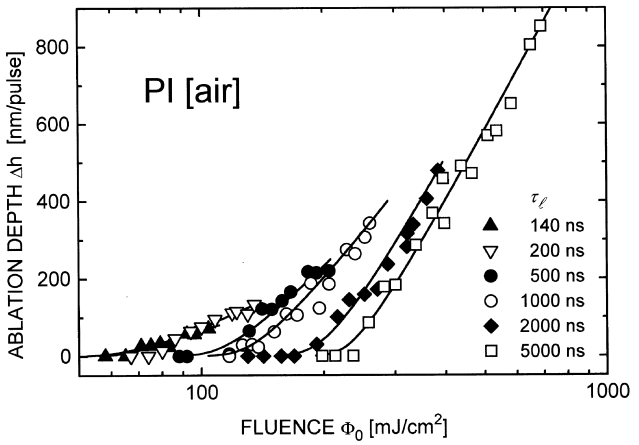

Fig. 3. Dependence of the ablation depth Δh on the incident fluence ϕ_0 (intensity I_0) for different (fixed) laser pulse lengths τ_l. The full curves were calculated using Eq. (1). The parameters employed were as follows: ▲, $A = 3.86 \times 10^8$ Å per pulse, $B = 0.908$ J cm^{-2}, $\alpha = 5.82 \times 10^4$ cm^{-1}; ▽, 5.51×10^8, 0.998, 4.21×10^4; ●, 6.89×10^8, 1.60, 1.95×10^4; ○, 1.38×10^9, 1.95, 1.59×10^4; ◆, 2.75×10^9, 2.98, 1.12×10^4; □, 2.75×10^{11}, 4.59, 1.12×10^4.

Clearly, a consideration of the temperature dependence of the material parameters may strongly influence this result. Of course, we can argue the other way around. If we calculate the maximum surface temperature for a certain pulse length τ'_l and (measured) threshold fluence $\phi_{th}(\tau'_l)$, and assume that ablation always starts at 1300 K, we obtain $\epsilon \approx 0.36$. If the intensity I_0 is fixed, we find $\phi_{th} \propto I_0^{-\delta}$ with $\delta \approx 0.43$. These data support the thermal mechanism, because the simple relation $\phi_{th}(\tau_l) = I(\tau_l)\tau_l$ yields $\phi_{th} \propto I^{-\delta}$ with $\delta = \epsilon/(1-\epsilon) \approx 0.56$, which is in reasonable agreement with the experimental value.

3.3. Fluences $\phi_0 > \phi_{th}$

A typical hole fabricated in a single-shot experiment with $\phi_0 > \phi_{th}$ is shown in Fig. 1(c). The dependence of the ablation depth on the fluence ϕ_0 (intensity I_0) for different (fixed) pulse lengths τ_l is shown in Fig. 3. The full curves were calculated on the basis of the interpolation formula [1]

$$\phi = B \exp[\alpha_0 \Delta h] \ln^{-1}\left[\frac{A}{\Delta h}\right] \quad (1)$$

where $B = \phi \Delta E / k_B T_{s,max}$. ΔE is the apparent activation energy. The maximum surface temperature $T_{s,max}$ can be calculated from the heat equation. α_0 describes the attenuation

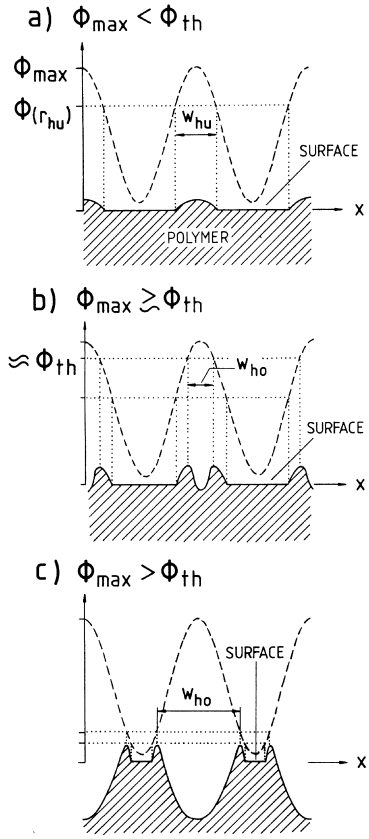

Fig. 4. Schematic drawing of the interference pattern $\phi(x)$ with $V = 0.9$ and period Λ (broken curve), and the corresponding topology changes on the polymer surface.

of the laser light within the vapour plume. A is related to the attempt frequency for desorption.

4. Interference gratings

The formation of interference gratings, as investigated in Ref. [17], can be interpreted on the basis of the surface morphology changes exhibited in Fig. 1. The broken curve in Fig. 4 shows the distribution of the fluence $\phi(x)$ caused by two interfering beams ϕ_i. If $\phi(x) \geq \phi(r_{hu})$, the surface is elevated. The width of the humps can be estimated from [12]

$$w_{hu} = 2r_{hu} = \frac{\Lambda}{\pi}\arccos\left\{\frac{[\phi(r_{hu})]/(2b\phi_i) - 1}{V}\right\} \quad (2)$$

where $k = 2\pi/\Lambda$ is the wavevector of the interference pattern, V is the visibility and b is a factor of the order of unity.

With $\phi(x) \geq \phi_{th}$, ablation takes place and will lead to hump splitting (Fig. 1(b) and Fig. 1(c)). If the maximum fluence of the interference pattern, ϕ_{max}, is further increased, neighbouring humps will almost merge and form double rows (Fig. 4(c)). This transition from single to double rows has been observed in Ref. [17].

5. Conclusions

Single-shot UV laser ablation ($\lambda \approx 302$ nm) of PI in air was investigated for laser pulse lengths of 140 ns $\leq \tau_l \leq 5$ μs and laser light intensities of $54 \leq I_0 \leq 430$ kW cm^{-2}. The depth of the holes generated by the laser light was measured by atomic force microscopy. Experiments were performed with either constant pulse length τ_l or constant intensity I_0. The ablation threshold ϕ_{th} increases with increasing pulse length ($\phi_{th} \propto \tau_l^{0.36}$) and decreases with increasing intensity ($\phi_{th} \propto I_0^{-0.43}$). The experimental results can be qualitatively interpreted on the basis of a thermal model and a (thermal or non-thermal) mechanism which decreases the apparent activation energy for the desorption of species from the surface. The formation of interference patterns and row doubling can be interpreted on the basis of the changes in surface topology observed.

Acknowledgements

We wish to thank Dr N. Arnold, Dr N. Bityurin and Professor B. Luk'yanchuk for valuable discussions and the Fonds zur Förderung der Wissenschaftlichen Forschung in Austria for financial support.

References

[1] D. Bäuerle, Laser Processing and Chemistry, Springer, Heidelberg, 1996.
[2] R. Srinivasan, in: J.C. Miller (Ed.), Laser Ablation: Principles and Applications, Springer, Heidelberg, 1994, p. 107.
[3] B. Luk'yanchuk, N. Bityurin, S. Anisimov, D. Bäuerle, Appl. Phys. A 57 (1993) 367.
[4] B. Luk'yanchuk, N. Bityurin, S. Anisimov, D. Bäuerle, Appl. Phys. A 57 (1993) 449.
[5] B. Luk'yanchuk, N. Bityurin, S. Anisimov, N. Arnold, D. Bäuerle, Appl. Phys. A 62 (1996) 397.
[6] R. Sauerbrey, G.H. Pettit, Appl. Phys. Lett. 55 (1989) 421.
[7] G.V. Treyz, R. Scarmozzino, R.M. Osgood Jr., Appl. Phys. Lett. 55 (1989) 346.
[8] R. Srinivasan, Appl. Phys. Lett. 58 (1991) 2895.
[9] R. Srinivasan, J. Appl. Phys. 72 (1992) 1651.
[10] M. Himmelbauer, E. Arenholz, D. Bäuerle, Appl. Phys. A 63 (1996) 87.
[11] M. Himmelbauer, E. Arenholz, D. Bäuerle, K. Schilcher, Appl. Phys. A 63 (1996) 337.
[12] M. Himmelbauer, N. Arnold, N. Bityurin, E. Arenholz, D. Bäuerle, Appl. Phys. A, (1997), in press.
[13] C. Feger, M.M. Khojasteh, J.E. McGrath, Polyimides: Materials, Chemistry and Characterization, Elsevier Science, Amsterdam, 1989.
[14] M.I. Bessonov, Poliimidy-Klass Termostoykikh Polimerov, Nauka Press, Leningrad, 1983.
[15] S. Küper, J. Brannon, K. Brannon, Appl. Phys. A 56 (1993) 43.
[16] P.E. Dyer, J. Sidhu, J. Appl. Phys. 57 (1985) 1420.
[17] H.M. Phillips, D.L. Callahan, R. Sauerbrey, G. Szabo, Z. Bor, Appl. Phys. A 54 (1992) 158.